Effect of Co doping on the electronic structure of $MgCNi_3$

I. R. Shein,[1] A. L. Ivanovskii,[1] E. Z. Kurmaev,[2] A. Moewes,[3] S. Chiuzbian,[4] L. D. Finkelstein,[2] M. Neumann,[4] Z. A. Ren,[5] and G. C. Che[5]

[1]*Institute of Solid State Chemistry, Russian Academy of Sciences-Ural Division, 620219 Yekaterinburg GSP-145, Russia*

[2]*Institute of Metal Physics, Russian Academy of Sciences-Ural Division, 620219 Yekaterinburg GSP-170, Russia*

[3]*Department of Physics and Engineering Physics, University of Saskatchewan, 116 Science Place, Saskatoon, Saskatchewan, Canada S7N 5E2*

[4]*Universität Osnabrück, Fachbereich Physik, D-49069 Osnabrück, Germany*

[5]*National Laboratory for Superconductivity, Institute of Physics, Chinese Academy of Sciences, P.O. Box 603, Beijing 100080, China*

(Received 14 January 2002; published 26 July 2002)

Self-consistent full-potential linear muffin-tin orbital band structure calculations of the antiperovskites $MgCNi_3$, $MgCNi_2Co$, and $MgCNiCo_2$ are presented. It is found that the electronic structure of $MgCNi_3$ near the Fermi level is dominated by a Ni $3d$-derived density of states peak just below the Fermi level, which provides the superconducting properties of this compound. The Co doping of $MgCNi_3$ is accompanied by a reduction of the density of states at the Fermi level, which seems to be responsible for the reduced superconductivity in the $MgCNi_{1-x}Co_x$ system. No magnetic solution is found for $MgCNi_2Co$ and $MgCNiCo_2$. This indicates that the hole doping does not produce the magnetic instability which can be responsible for pair breaking. The validity of the band structure calculations is confirmed by x-ray emission (C $K\alpha$, Ni $L_{2,3}$, and Co $L_{2,3}$) and x-ray photoelectron spectra measurements of superconducting $MgC_{1.45}Ni_3$ ($T_c=7.5$ K) and nonsuperconducting $MgC_{1.45}Ni_{1.5}Co_{1.5}$.

DOI: 10.1103/PhysRevB.66.024520 PACS number(s): 74.70.Ad, 78.70.En, 74.62.Dh, 74.25.Jb

I. INTRODUCTION

The recent discovery of superconductivity in the intermetallic perovskite $MgCNi_3$ Ref. 1 has provided a link between two major families of superconducting materials: the intermetallic compounds and the perovskite-based oxides. The observation of superconductivity in $MgCNi_3$ is surprising given the large amount of nickel present, an element usually associated with magnetism. $MgCNi_3$ forms a three-dimensional perovskite structure. Mg, C, and Ni replace Sr, Ti, and O in $SrTiO_3$, respectively. Six Ni atoms at the face-centered position of each cubic unit cell of $MgCNi_3$ form a three-dimensional network of Ni_6 octahedra similar to oxygen octahedra in $SrTiO_3$. This is very unusual because in this case nickel atoms occupy anion positions in the perovskite structure, while Ni usually is an electron donor. Therefore $MgCNi_3$ is often referred to as a compound with an antiperovskite structure.

The $MgCNi_3$ band structure displays a characteristic very large and narrow energy peak in the density of states (DOS) just below the Fermi energy.[2–7] This type of narrow energy peak is typical for materials that display strong magnetic interactions. It suggests that hole doping (Co) should induce a transformation from superconducting to magnetic. Electron doping (Cu), on the other hand, should lead to a decrease in T_c simply due to a decreasing density of states.

Experiments have shown that substituting Ni sites doping with Co and Cu leads to a decrease in T_c.[7] However, no evidence for long-range magnetic ordering has been observed in the magnetic susceptibility of the Co-doped material.[7] Therefore a theoretical study of the effect of Co doping on the electronic structure of $MgCNi_3$ as well as experimental verification of band structure calculations is of great interest.

In the present paper we study the theoretical effect of Co doping on the electronic structure of $MgCNi_3$ using the linearized muffin-tin orbital (LMTO) band method in the local density approximation. In order to verify the results experimentally, x-ray emission and x-ray photoelectron measurements of superconducting $MgC_{1.45}Ni_3$ ($T_c=7.5$ K) and nonsuperconducting $MgC_{1.45}Ni_{1.5}Co_{1.5}$ are presented. Nonresonant carbon $K\alpha$ ($2p\rightarrow 1s$ transition), nickel $L_{2,3}$, and cobalt $L_{2,3}$ ($3d4s\rightarrow 2p$ transition) x-ray emission spectra (XES) probe directly the distribution of occupied C $2p$, Ni $3d4s$, and Co $3d4s$ partial density of states, respectively.

II. CALCULATION AND EXPERIMENTAL DETAILS

We have used a scalar relativistic self-consistent full-potential LMTO method within the local density approximation (LDA).[8,9] The correlation and exchange effects and relativistic effects are taken into account using the generalized gradient approximation (GGA).[10] The tetrahedron method was used to calculate the DOS with 550 irreducible **k** points. In the crystal structure of cubic $MgCNi_3$ (cubic, perovskite type, $Pm3m$ space group) the atoms occupy the positions 3Ni (0;1/2;1/2), Mg (0;0;0), and C (1/2;1/2;1/2). The theoretical equilibrium lattice parameter of $MgCNi_3$ ($a=3.8137$ Å) was obtained by minimization of the total energy, which is in good agreement with the experimental equilibrium for $MgC_{0.96}C$ ($a=3.8122$ Å).[11] We have used the same lattice parameter for all Co-doped $MgCNi_3$ compounds because the changes in the lattice parameter from $MgC_{1.45}Ni_3$ to $MgC_{1.45}Co_3$ are found to be negligible.[12] We have performed supercell calculations for ordered $MgCNi_{3-x}Co_x$ ($x=1$ and 2).

In the sample preparation fine powders of Mg, C, Ni, and Co with purity better than 99.5% were used as starting materials. The mixture with appropriate composition was pressed into pellets. The pellets were wrapped with Ta foil

and enclosed in an evacuated quartz tube, then placed in a box furnace and heated to 950 °C at a rate of 150 °C/h and kept at this temperature for 5 h, followed by furnace cooling to room temperature. It is observed that the T_c of MgC_xNi_3 is sensitive to the carbon content. The highest T_c corresponds to $x=1.45$.[12] For $x=1.55$ the transition temperature in MgC_xNi_3 decreases to $T_c=5.3$ K. Under Co doping of $MgC_{1.45}Ni_{3-y}Co_y$ the superconducting transition temperature decreases gradually with increasing y and completely suppressed at $y=1.5$.[12]

The carbon $K\alpha$ ($2p\rightarrow 1s$ transition) and nickel (cobalt) $L_{2,3}$ ($3d4s\rightarrow 2p$ transition) soft XES were measured at Beamline 8.0 of the Advanced Light Source at Lawrence Berkeley National Laboratory employing the x-ray fluorescence endstation.[13] The excitation energy of the incident photons is taken as 300, 770, and 845 eV for measurements of C $K\alpha$, Co $L_{2,3}$, and Ni $L_{2,3}$ XES, respectively. Carbon $K\alpha$ spectra were measured with an energy resolution of 0.3 eV; for cobalt and nickel $L_{2,3}$ XES, the energy resolution is 0.7–0.8 eV.

The x-ray photoemission spectroscopy (XPS) measurements were performed with an ESCA spectrometer of Physical Electronics [PHI 5600 ci, with monochromatized Al $K\alpha$ radiation of a 0.3 eV full width at half maximum (FWHM)]. The energy resolution of the analyzer was 1.5% of the pass energy. The pressure in the vacuum chamber during the measurements was below 5×10^{-9} mbar. Prior to XPS measurements the samples were fractured in ultrahigh vacuum. All photoemission studies were performed at room temperature on freshly cleaved surfaces. The XPS spectra were calibrated using a Au foil to obtain photoelectrons from the Au $4f_{7/2}$ subshell. The binding energy for Au $4f_{7/2}$ electrons is 84.0 eV.

III. RESULTS AND DISCUSSION

A. Band structure calculations

Figures 1–3 display band structure calculations for $MgCNi_3$, $MgCNi_2Co$, and $MgCNiCo_2$. The valence band (VB) of undoped $MgCNi_3$ (Fig. 1) consists of three bands (labeled *A*, *B*, and *C*). Mg, C, and Ni states contribute to the lowest band (*A*). Its lowest edge is formed by C $2s$ states, whereas Ni $3d$ and Mg $2p$ states reside at the top. The *B* band is dominated by Ni $3d$ states. To some extent Mg $3p$ states mix with Ni $3d$ states at the bottom. The most striking feature of the Ni DOS is the strong and narrow peak *C* located ~80 meV below the Fermi level. This is in accordance with other band structure calculations available,[2–7] and it is characteristic for materials that display strong magnetic interactions. It is supposed that $MgCNi_3$ is close to magnetic instability and hence hole doping should induce a transition from superconductivity to magnetism. According to estimations,[5] the Stoner exchange parameter *S* defined as $S=N(E_F)I_{XC}$ (where I_{XC} is the intra-atomic exchange-correlation integral) is $S=0.64$. Therefore hole doping, which can be realized by replacing Ni with Co, will yield a Stoner parameter larger than 1 and can induce the magnetic instability. However, no magnetic instabilities are found in our band structure calculations of $MgCNi_2Co$ and $MgCNiCo_2$, which is in accordance with magnetic susceptibility measurements for $MgCNi_{3-x}Co_x$ (Ref. 7) according to which no signature of long magnetic ordering has been observed in this system. According to the calculated total and partial DOS at E_F, substitution of Ni with Co in $MgCNi_3$ leads to a reduction in the density of states at the Fermi level from 4.665 (for $MgCNi_3$) to 3.651 (for $MgCNi_2Co$) and 0.961 states/eV (for $MgCNiCo_2$). This behavior can be responsible the observed reduction in superconductivity associated with Co doping.

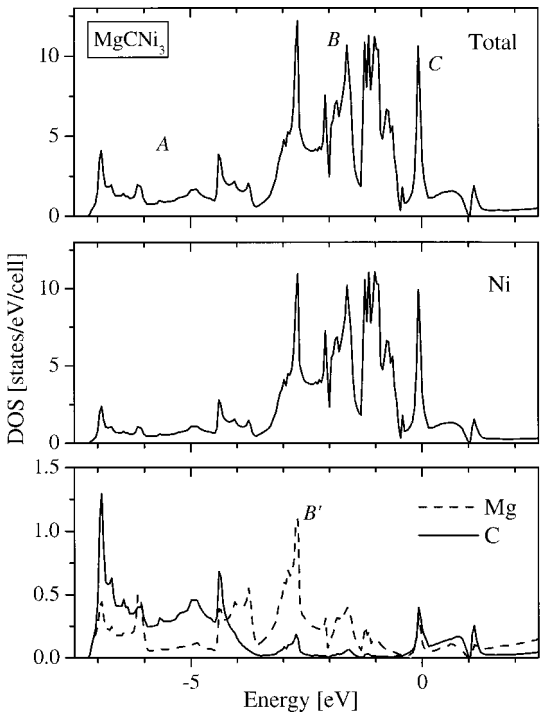

FIG. 1. Total and partial DOS for $MgCNi_3$.

Figures 2 and 3 show the calculated total and partial DOS for $MgCNi_2Co$ and $MgCNiCo_2$. A reduction of the *C* peak height and a shift of the Fermi level are evident, and both are likely due to a decrease in electron concentration. As a result, π^*-antibonding states become unoccupied for $MgCNiCo_2$ and the Fermi level is located in the pseudogap. The reduction of superconducting properties of $MgCNi_3$ under Co doping can be attributed to the redistribution of the electronic states in the vicinity of the Fermi level. The calculations suggest a substantial decrease in the density of states at the Fermi level with increasing Co content.

B. X-ray emission and photoelectron spectra

Figure 4 presents C $K\alpha$, Co $L_{2,3}$, and Ni $L_{2,3}$ soft XES measurements of $MgC_{1.45}Ni_3$, $MgC_{1.55}Ni_3$, and $MgC_{1.45}Ni_{1.5}Co_{1.5}$. Carbon *K* emission (top graph) probes the occupied C $2p$ states and shows a fine structure that is consistent with the calculated C $2p$ DOS for $MgCNi_3$ (Fig. 1). The variation of carbon content in MgC_xNi_3 does not change the intensity distribution of C $K\alpha$ XES.

Ni $L_{2,3}$ XES (Fig. 4, middle graph) is measured with less energy resolution than C $K\alpha$ XES, and therefore it is diffi-

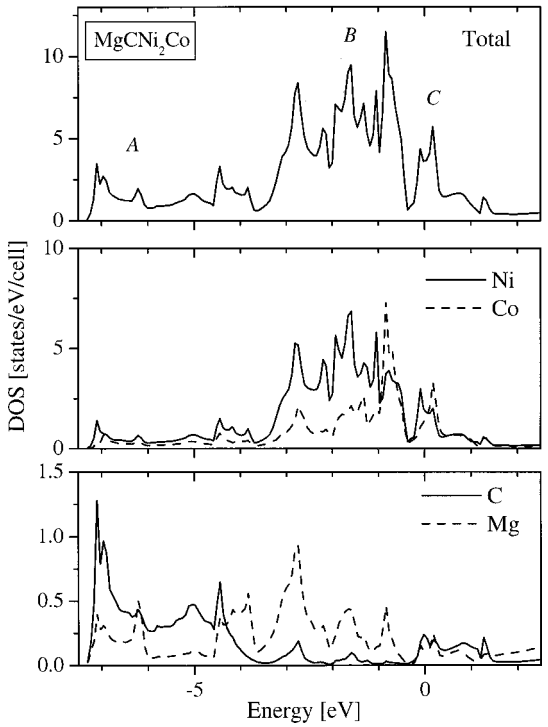

FIG. 2. Total and partial DOS for $MgCNi_2Co$.

cult to verify details of the Ni $3d4s$ DOS in the valence band of $MgCNi_3$ as shown in Fig. 1 from the experiment. On the other hand, we can compare the ratio of $I(L_2)/I(L_3)$ in $MgC_{1.45}Ni_3$, $MgC_{1.45}Ni_{1.5}Co_{1.5}$, and pure Ni and determine chemical and valence state of Ni atoms in these intermetallic perovskites. $L_{2,3}$ XES corresponds to dipole transition $3d4s \rightarrow 2p_{1/2,3/2}$, and the ratio of the L_2 to L_3 emission lines

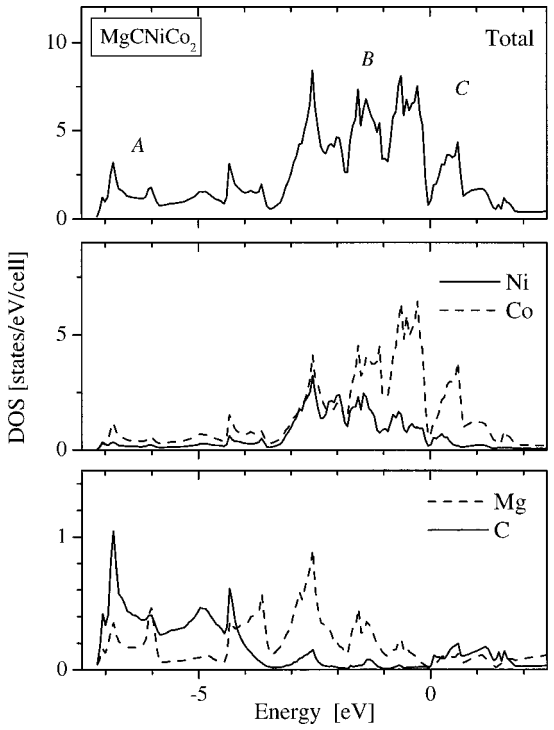

FIG. 3. Total and partial DOS for $MgCNiCo_2$.

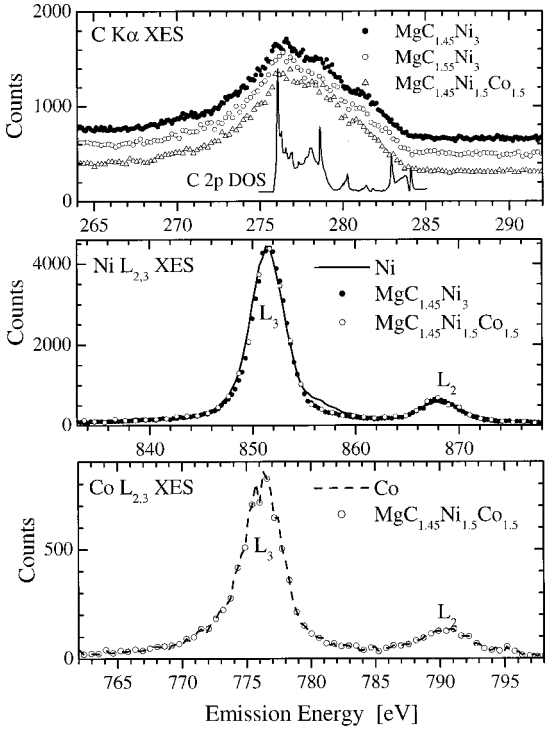

FIG. 4. C $K\alpha$, Ni $L_{2,3}$, and Co $L_{2,3}$ XES in $MgCNi_3$ and related compounds.

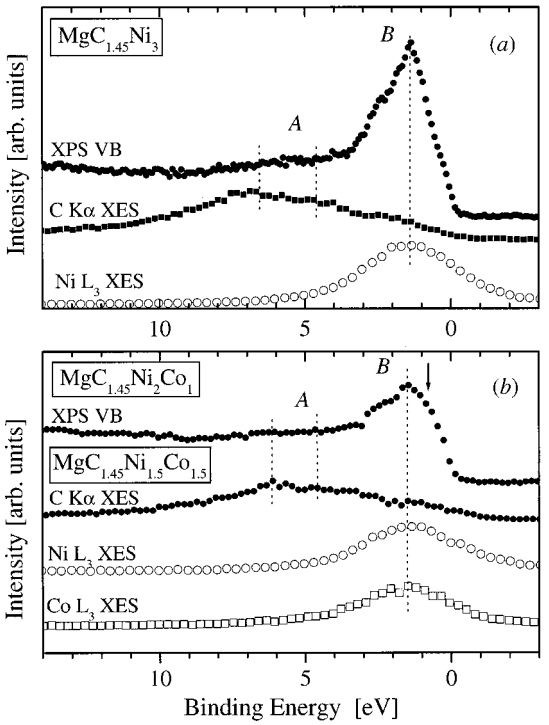

FIG. 5. Comparison of XPS VB's of $MgC_{1.45}Ni_3$ (a) and $MgC_{1.45}Ni_2Co$ (b) with x-ray emission spectra of constituents for $MgC_{1.45}Ni_3$ and $MgC_{1.45}Ni_{1.5}Co_{1.5}$ on the common binding energy scale.

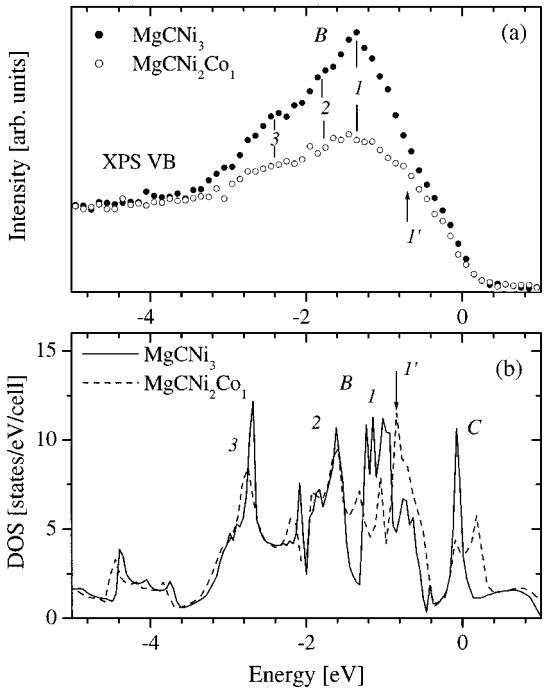

FIG. 6. XPS VB's (a) and total DOS (b) of $MgCNi_3$ and $MgCNi_2Co$.

$I(L_2)/I(L_3)$ should be the same for all $3d$ elements and close to the statistical value of $\frac{1}{2}$. However, it is found that this ratio is much less in pure $3d$ metals due to strong Coster-Kronig processes of the kind $L_2L_3M_{4,5}$.[14,15] The probability for nonradiative $L_2L_3M_{4,5}$ Coster-Kronig transitions is lower for $3d$ oxides than for metals[16] due to the localized character of d states and the absence of electron-hole pairs near the Fermi level as well as collective $3d$ electron excitations.[17] It is shown that the $I(L_2)/I(L_3)$ ratio can be used as a tool for determination of metallic state of $3d$ atoms in compounds under metal-insulator transitions.[18] The Ni $L_{2,3}$ XES displays the same ratio $I(L_2)/I(L_3)$ for $MgC_{1.45}Ni_3$, $MgC_{1.45}Ni_{1.5}Co_{1.5}$, and pure Ni. The same behavior is observed for Co $L_{2,3}$ XES in $MgC_{1.45}Ni_{1.5}Co_{1.5}$ where XES, the $I(L_2)/I(L_3)$ ratio, is also found to be close to that in pure Co (Fig. 4, bottom). This means that in antiperovskite structure Ni (or Co) atoms occupying the positions of oxygen in typical perovskites such as $SrTiO_3$ are not negatively charged, but remain in their metallic state as in intermetallic compounds. This is consistent with Ref. 2, which states that the crystal structure of $MgCNi_3$ may be conceptually viewed as expanded fcc Ni with 25% of the sites replaced by Mg and C interstitials in octahedral sites. This results in narrow and transition metal-like bands around the Fermi level with a higher filling than in pure Ni.[4] According to Hall effect measurements,[19] the carriers in $MgCNi_3$ are electrons, but not holes as in the superconducting oxide perovskites.

The comparison of XPS measurements of the VB of $MgC_{1.45}Ni_3$ and $MgC_{1.45}Ni_2Co$ (probing the total DOS) with x-ray emission spectra of constituents (C $K\alpha$, Ni L_3, and Co L_3 XES) of $MgC_{1.45}Ni_3$ and $MgC_{1.45}Ni_{1.5}Co_{1.5}$ which probe partial DOS is presented in Fig. 5 on the binding energy scale. In order to convert C $K\alpha$, Ni L_3, and Co L_3 XES to the binding energy scale we have used XPS C $1s$ (284.4 eV), Ni$2p_{3/2}$ (853 eV), and Co $2p_{3/2}$ (778.3 eV) binding energies. In good agreement with our band structure calculations of $MgCNi_3$, the carbon $2p$ states are located at the bottom of the valence band (A), whereas Ni L_3 emission coincides with the main peak (B) of the XPS VB situated near the Fermi level. Figure 5(b) suggests that Co doping leads to the formation of an additional maximum (indicated by arrow) in the valence band. This maximum is not observed in the Co L_3 emission due to insufficient energy resolution. We note that Co L_3 XES is located very close on the binding energy scale to Ni L_3 XES. We have compared XPS VB's of $MgC_{1.45}Ni_3$ and $MgC_{1.45}Ni_2Co$ in Fig. 6 by normalizing to the intensity of the carbonlike bands because both compounds have the same carbon content. Using this procedure, we can compare the d-band structure of $MgC_{1.45}Ni_2Co$ and $Mg_{1.45}CNi_3$ in the most intense region B of the XPS VB. Taking into account that the Ni $3d$ subshell has a 1.6 times larger atomic cross section than the Co $3d$ subshell for Al $K\alpha$ radiation,[20] we conclude that the reduction in intensity of the XPS B band under Co doping is due to a decrease in concentration of the Ni content and the formation of Co $3d$-derived peaks in the valence band of $MgC_{1.45}Ni_2Co$. The comparison of the XPS VB's of undoped and Co-doped $MgCNi_3$ shows that for doped compounds the intensities of the subpeaks (1–3) are reduced, but on the other hand, the additional maximum ($1'$) appears near the Fermi level. The same behavior is observed when comparing the calculated total DOS for $MgCNi_2Co$ and $MgCNi_3$ in Fig. 6(b). The additional subpeak ($1'$) has higher contributions from the Co $3d$ local DOS, whereas for the remaining subpeaks (1–3) the Ni $3d$ contribution prevails. The local Ni $3d$ DOS decreases along the B band towards to the Fermi level (Fig. 2). Contrary to this, the Co $3d$ DOS increases in the same direction. The center of gravity of Ni $3d$-occupied states is found to be located deeper than the Co $3d$ states with respect to the Fermi level. Therefore the B band in $MgCNi_2Co$ is a result of the superposition of Ni $3d$ and Co $3d$ local DOS with Ni $3d$ states at the bottom and Co $3d$ states at the top.

Our band structure calculations of $MgCNi_3$ and $MgCNi_2Co$ are in reasonable agreement with the experimental spectra. Based on these calculations, we can conclude that Co doping of $MgCNi_3$ leads to a decrease in density of states at the Fermi level which can induce the reduction of superconductivity in $MgCNi_{3-x}Co_x$ systems.

IV. CONCLUSION

To conclude, we have studied the effect of Co doping on the electronic structure of $MgCNi_3$ by using self-consistent LMTO band structure calculations and x-ray emission and photoelectron measurements. We have found that the total occupied $3d$ density of states of $MgCNi_{3-x}Co_x$ can be described as a superposition of Ni $3d$ and Co $3d$ local DOS. Spin-polarized band structure calculations have shown that hole doping of $MgCNi_3$ does not induce magnetic instabilities. Substitution of Ni with Co in $MgCNi_{3-x}Co_x$ is accompanied by a decrease in the density of states at the Fermi

level. This decrease can be responsible for the suppression in superconductivity of this system.

ACKNOWLEDGMENTS

This work was supported by the Russian State Program on Superconductivity, the Russian Foundation for Basic Research (Project No. 00-15-96575), the National Sciences and Engineering Research Council (NSERC), the Minister of Science and Technology of China (NKBRSF-G 19990646), and the NATO Collaborative Linkage Grant (PST.CLG.978044). The work at the Advanced Light Source at Lawrence Berkeley National Laboratory was supported by the U.S. Department of Energy (Contract No. DE-AC03-76SF00098).

[1] T. He *et al.*, Nature (London) **411**, 6833 (2001).
[2] D. J. Singh and I. I. Mazin, Phys. Rev. B **64**, 140507 (2001).
[3] A. Szajek, J. Phys.: Condens. Matter **13**, L595 (2001).
[4] S. B. Dugdale and T. Jarlborg, Phys. Rev. B **64**, 100508 (2001).
[5] J. H. Shim, S. K. Kwon, and B. I. Min, Phys. Rev. B **64**, 180510(R) (2001).
[6] I. R. Shein, A. L. Ivanovskii, and N. I. Medvedeva, Pis'ma Zh. Eksp. Teor. Fiz. **74**, 127 (2001) [JETP Lett. **74**, 127 (2001)].
[7] M. A. Hayward *et al.*, Solid State Commun. **119**, 491 (2001).
[8] M. Methfessel and M. Scheffler, Physica B **172**, 175 (1991).
[9] S. Y. Savrasov, Phys. Rev. B **54**, 16 470 (1996).
[10] J. P. Perdew and Y. Whang, Phys. Rev. B **45**, 13 244 (1992); J. P. Perdew, S. Burke, and M. Ernzerhof, Phys. Rev. Lett. **77**, 3865 (1996).
[11] Q. Huang, T. He, K. A. Regan, R. Rogado, M. Hayward, M. K. Haas, K. Inumaru, and R. J. Cava, cond-mat/0105240 (unpublished).
[12] Z. A. Ren, G. C. Che, S. L. Jia, H. Chen, Y. M. Ni, and Z. X. Zhao, cond-mat/0105366 (unpublished); Sci. China, Ser. A: Math., Phys., Astron. Technol. Sci. **44**(9), 302 (2001).
[13] J. J. Jia, T. A. Callcott, J. Yurkas, A. W. Ellis, F. J. Himpsel, M. G. Samant, J. Stöhr, D. L. Ederer, J. A. Carlisle, E. A. Hudson, L. J. Terminello, D. K. Shuh, and R. C. C. Perera, Rev. Sci. Instrum. **66**, 1394 (1995).
[14] E. J. McGuire, Phys. Rev. A **5**, 1043 (1972).
[15] J. E. Holliday, J. Appl. Phys. **33**, 3259 (1962).
[16] V. R. Galakhov, E. Z. Kurmaev, and V. M. Cherkashenko, Izv. Akad. Nauk SSSR, Ser. Fiz. **49**, 1513 (1985).
[17] V. I. Grebennikov, V. R. Galakhov, L. D. Finkelstein, N. A. Ovechkina, and E. Z. Kurmaev (unpublished).
[18] A. Moewes, E. Z. Kurmaev, L. D. Finkelstein, A. V. Galakhov, J. P. Rueff, and C. F. Hague (unpublished).
[19] S. Y. Li, R. Fan, X. H. Chen, C. H. Wang, W. Q. Mo, K. Q. Ruan, Y. M. Xiong, X. G. Luo, H. T. Zhang, L. Li, Z. Sun, and L. Z. Cao, Phys. Rev. B **64**, 132505 (2001).
[20] J. J. Yeh and I. Lindau, At. Data Nucl. Data Tables **32**, 1-155 (1985).